The Poulos−Kraut Mechanism of Compound I Formation in Horseradish Peroxidase: A QM/MM Study

Etienne Derat and Sason Shaik*

Department of Organic Chemistry and the Lise Meitner-Minerva Center for Computational Quantum Chemistry, Hebrew University of Jerusalem, Givat Ram Campus, 91904 Jerusalem, Israel

Received: September 23, 2005; In Final Form: March 30, 2006

QM/MM calculations are used to elucidate the Poulos−Kraut (Poulos, T. L.; Kraut, J. *J. Biol.* Chem. **1980**, *255*, 8199−8205) mechanism of O−O bond activation and Compound I (Cpd I) formation in HRP, in conditions corresponding to neutral to basic pH. Attempts to generate Compound I directly from the Fe(H_2O_2) complex by migrating the proton from the proximal oxygen to the distal one (1,2- proton shift) result in high barriers. The lowest energy mechanism was found to involve initial deprotonation of ferric hydrogen peroxide complex (involving spin crossover from the quartet to the doublet state) by His42 to form ferric-hydroperoxide (Cpd 0). Subsequently, the distal OH group of Cpd 0 is pulled by Arg38 and reprotonated by His42(H^+) to form Cpd I and a water molecule that bridges the two residues. The structures of the intermediate and the transition state reveal the manner by which the Arg−His residues promote cooperatively the electronic reorganization that is required to attend the heterolytic O−O cleavage.

Introduction

O−O bond activation in heme enzymes is one of the important processes in nature, crucial for terrestrial life.[1−7] In heme peroxidases this process, shown in Scheme 1, involves binding of hydrogen peroxide followed by O−O bond activation and formation of the primary active species, Compound I (Cpd I). The latter species stores two oxidation equivalents, which are used subsequently for substrate oxidation, thereby leading to vital functions. Understanding the mechanism of Cpd I formation is one of the intellectual challenges in heme enzymes.[1−4,7]

A commonly accepted mechanism for peroxidases is the Poulos−Kraut mechanism[6] that involves acid−base catalysis, through the highly conserved His−Arg couple in the distal side, resulting in heterolytic cleavage of the O−O bond. Nevertheless, the molecular details of this process are not yet fully established (Scheme 1). This is especially true for the unstable intermediates along the path. There seem to be three types of intermediate candidates, which depend on pH and which appear in the wild type and different distally mutated peroxidases.[7] One potential intermediate appears to be the Fe(H_2O_2) complex, and the second one is Compound 0 (Cpd 0), namely, the Fe−OOH species that is formed by deprotonation of the hydrogen peroxide, e.g., by the distal His residue that acts as a base. A third potential intermediate is the Fe−OOH_2 species that arises by reprotonation of the distal oxygen (O_β) of FeOOH. Due to the difficulties of identifying these unstable and short-lived intermediates by experimental means,[1,7] their existence and roles in the formation of Cpd I are not certain. Other issues concern the more precise functions of the distal residues, His and Arg; do both participate as a base−acid couple, or is it only His that is responsible for the formation of Cpd I? And if indeed only His matters, then what is the precise role of the Arg residue? Additional difficulties derive from the available spin state situations of the species involved in Scheme 1. Thus, while Cpd I has two virtually degenerate spin states, doublet and quartet,[8] the other species in Scheme 1 have three closely lying spin states: doublet, quartet, and sextet.[9,10] Deciphering the mechanisms for all the states is therefore called for.

Theoretical calculations can provide the requisite information and elucidate the mechanism of Cpd I formation. Most of the current theoretical treatments (on peroxidases), known to us, have been carried on the isolated heme molecule,[8−12] and while these studies led to valuable results including the spectral characterization of the Cpd 0 and Fe(H_2O_2) intermediates in Scheme 1,[9b] the questions posed above regarding the O−O activation mechanism require the type of calculation that takes into account the entire active site, or at least the key residues that are involved in the process.[12a,b,13] The hybrid quantum mechanical/molecular mechanical (QM/MM) method fulfills this requirement since it calculates the enzymatic species within their native protein.

In a recent paper, we used QM/MM calculations to describe the structure and spectroscopy of the active species Cpd I of the enzyme horseradish peroxidase (HRP), in Figure 1.[14] One of the conclusions of the study was that the distal residues, His42 and Arg38 are essential and have to be included in the QM subsystem for reproducing structural and Mössbauer spectroscopic features for this species.[15,16] Especially important for the Mössbauer parameters was the hydrogen bonding network leading from the oxo group of Cpd I through the crystalline water molecule (W427) and the doubly protonated His42−H^+. In the present work we use QM/MM calculations to decipher the mechanism of O−O bond activation that leads to the formation of Cpd I for HRP, in neutral to basic pH.[7] The specific functions of the two key distal residues and the formation of bridging water molecule will clearly emerge from our study, along with insight into the roles of these groups in promoting the electronic reorganization needed to convert a ferric species

* Corresponding author. Tel +972 (0)2 658 5909, Fax +972 (0)2 658 4033, E-mail: sason@yfaat.ch.huji.ac.il

10.1021/jp055412e CCC: $33.50
Published on Web 05/06/2006

SCHEME 1: Schematic Description of the Mechanism for the Formation of Compound I in Presence of H_2O_2 (question marks signify putative intermediates).

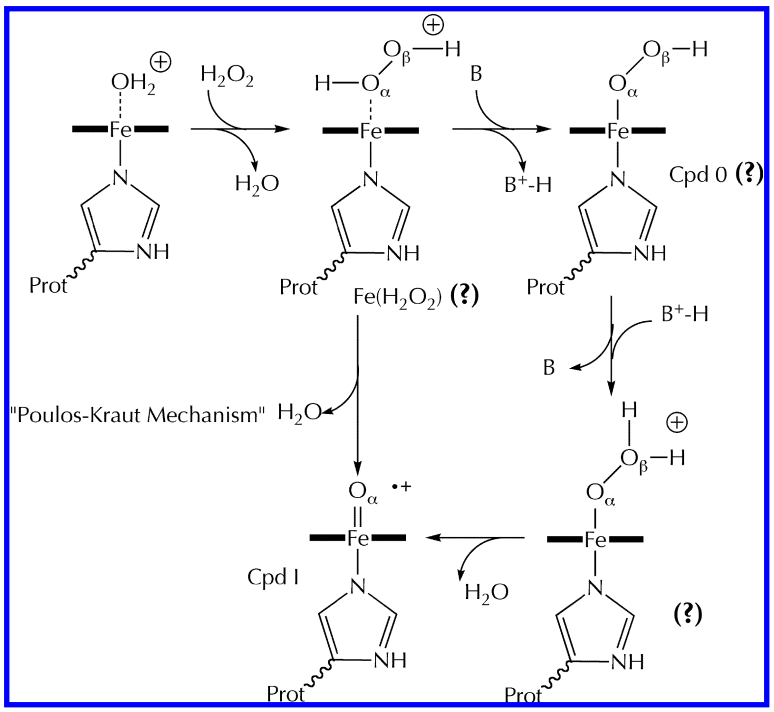

(Fe(III)) to a high-valent ferryl-oxo porphyrin radical cationic state (Por+•Fe(IV)═O). The roles of different spin states will also be clarified by the computational results.

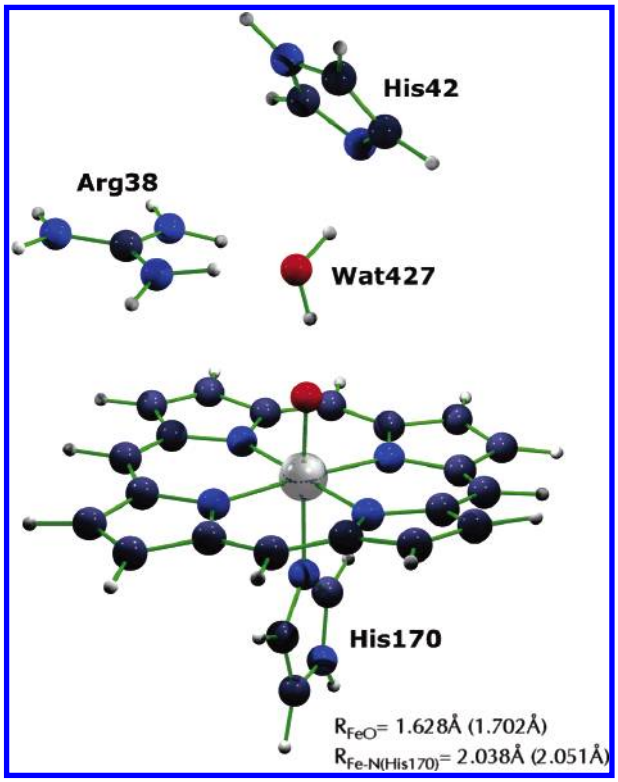

Figure 1. Structure of HRP Compound I obtained by QM/MM calculations (UB3LYP/B1+(d):CHARMM). The labeling corresponds to PDB 1HCH, which was used for the setup. The geometric data outside of the parentheses correspond to the present study, where the histidine (His42) is nonprotonated in the end of the process (described in Figures 2-4), corresponding to neutral pH, whereas the values in parentheses correspond to the results reported in ref 14, in which the His42 was used in its doubly protonated form (see Supporting Information Figure S.1).

Computational Methods

A. QM/MM Methodology and Software. The QM/MM method[17,18] divides the total enzyme into two subsystems, the active center and the remaining parts, comprising the protein, ions, crystal water, and surface water. The active center is treated by a quantum mechanical (QM) method, which, in the present case, is the unrestricted UB3LYP functional of density functional theory (DFT). The remaining parts are all treated by molecular mechanics (MM), using a protein force field. The two subsystems are allowed to interact by electrostatic and van der Waals type terms, such that after optimization, the QM subsystem adapts its geometry, electronic structure, and charge distribution to the polarity and steric constraints of the protein environment, and to its hydrogen bonding machinery.

Since the QM subsystem is extracted from the protein, the dangling bonds at the boundary have to be handled specifically. In the present study we use the electrostatic embedding method that incorporates the MM charges into the one electronic Hamiltonian of the QM procedure, while the dangling bonds are capped with H-atoms (the link atom method) and the effect of this replacement is corrected by the charge shift method.[19] The QM/MM calculations are performed with the ChemShell software[20] that integrates the TURBOMOLE package for QM,[21] and the DL-POLY program,[22] which uses the CHARMM22 force field,[23] for MM.

Four basis sets were used in the study, B1, B1+(d), B2, and B3: B1 consists of an effective core potential on iron coupled with the double ζ basis set; LACVP,[24] and 6-31G on all other atoms. B1+(d) augments the oxygen atoms with polarization and diffuse functions, relative to B1. B2 describes the iron by the Wachters all electron basis set[25] augmented with diffuse d and f polarization functions; the first coordination sphere of iron and other electronegative atoms are represented by 6-31+G-(d), while the remaining atoms by 6-31G(d). To estimate the acidity of the $Fe(H_2O_2)$ complex, and its mode of conversion to Cpd 0, we also used B3 which corresponds to B2 augmented

by diffuse and polarization functions on hydrogens (6-31++G-(d,p)). As such, the B3 basis set is balanced in the treatment of all atoms.

B. Setup of the System. We started from the experimental X-ray structure of HRP Cpd I,[15] reported by Berglund et al. (PDB code: 1HCH). A complete model of the solvated enzyme was built by adding the missing hydrogen atoms and a 16 Å-thick water solvent layer. The complete system consisted of 19452 atoms, including 13395 atoms in the solvent.

The total charge of the so-generated system was zero and corresponded to the following protonated state of the various residues: Aspartates (Asp) and glutamates (Glu) are negatively charged (Asp 8, 20, 29, 43, 50, 56, 66, 81, 99, 125, 132, 150, 162, 182, 194, 220, 222, 230, 247, 258, 282; Glu 25, 64, 88, 238, 239, 249, 279), and arginines (Arg) and lysines (Lys) are positively charged (Arg 19, 27, 31, 38, 62, 75, 82, 93, 118, 123, 124, 153, 159, 178, 183, 206, 224, 264, 283, 298, 302; Lys 65, 84, 149, 174, 232, 241). One more positive charge is "located" on the heme moiety. The histidines (His40, His42, His170) were singly protonated, and hence electrically neutral. Of these His residues, one is the proximal ligand His170, the other is the distal residue His42 that was kept neutral to represent the situation in neutral to basic pH.

This above system was then relaxed by means of force field energy minimization and short molecular dynamics (MD) simulations, using the CHARMM22 force field, keeping fixed the coordinates of the heme unit and the histidine ligand, His170 (Figure 1). The MD calculations did not significantly modify the structure vis-à-vis the initial X-ray structure.[14] Therefore, we ran the QM/MM calculations on the coordinates obtained after the force field energy minimization and short MD on the inner solvent layer (to remove close contacts).

C. The Optimized QM/MM Region. In addition to the QM region (see below) the QM/MM geometry optimization included the following residues: Arg_{31}, Ser_{35}, Arg_{38}, Phe_{41}, His_{42}, Ser_{73}, Leu_{138}, Pro_{139}, Ala_{140}, Pro_{141}, Ser_{167}, His_{170}, Gln_{176}, Ile_{244}, Asp_{247}, Phe_{221}, Tyr_{233}, W_{427}, W_{423}, W_{278}.

D. The QM Region. Based on previous study of Cpd I (see Figure 1),[14] using the same methodology, the mechanism was investigated using a QM subsystem comprising of the heme with its distal ligand (e.g., H_2O_2), Arg38, His42, and Wat427 (the latter originates from the ultimate activation of H_2O_2). Our study does not involve supply of extra protons, and consequently, the end point of the mechanism leaves His42 as a neutral species with a single proton (See Figure 1). However, since His42 is near the surface, we assume it can easily be protonated to generate the Cpd I species from our previous computations,[14] where the W427 and the doubly protonated His42 cause FeO bond elongation and some spin density rearrangement, which were important for the Mössbauer parameters. Thus, the previously calculated Cpd I species represents the situation of Cpd I in an acidic conditions, while the one generated in this study represents Cpd I as it would be in neutral or slightly basic conditions.[7b]

E. Mechanisms of Deprotonation or Rearrangment of H_2O_2. We have made many attempts to search for low energy mechanisms that cause deprotonation of H_2O_2 in the ferric complex, or its rearrangement to the ferric−water oxide complex ($FeO-OH_2$, in Scheme 1). All these attempts are summarized in the Supporting Information document (SI) in pages S.37−S.40.

Results and Discussion

Reaction Intermediates. The first potential intermediate is a complex of HRP with H_2O_2. Three spin-states, doublet, quartet, and sextet were investigated and found to be genuine minima on the potential energy surface. Figure 2 shows the lowest states, of doublet and quartet spin, while key geometric data for the sextet spin state are presented in Figure 4 and are discussed below (see also the Supporting Information pages S6, S7, and S20). The most tightly bonded species is the doublet state. In this state, the complex possesses a single unpaired electron localized in a π^* like orbital (spanning Fe, O_α and O_β), the distance between iron and the proximal oxygen (O_α) is 2.233 Å. In the closely lying quartet spin state (0.5 kcal/mol above the doublet with UB3LYP/B2//B1+d), there are three unpaired electrons, two in π^*-type orbitals and one in the $\sigma^*(z^2)$ orbital that possesses antibonding interactions across the Fe−O and the $Fe-N_{His170}$ linkages. The distance between iron and oxygen is 2.467 Å, reflecting the antibonding character of the $\sigma^*(z^2)$ orbital along the Fe−O *z*-axis. A still longer Fe−O bond is possessed by the sextet state species, ca. 2.623 Å; this state is, however, high lying for Cpd I and was not considered any longer. In all the three $Fe(H_2O_2)$ species, the hydrogen peroxide moiety is clamped to the distal residues.[6,7] Figure 2 shows this hydrogen-bonding network for the doublet and quartet spin states. It is seen that His42 and Arg38 hold the hydrogen peroxide ligand in a double donor−acceptor fashion; one H-bond is donated by H_2O_2 to His42, the other is accepted by H_2O_2 from Arg38 (see Supporting Information pages S6−S7 and S18−S19).

When a proton is abstracted from H_2O_2, this generates a ferric hydroperoxide Fe−OOH complex, the so-called Cpd 0 intermediate species. The calculations show that, as expected,[10,12a] Cpd 0 has a doublet spin ground state; the quartet spin state is 6.6 kcal/mol higher (the B2//B1+(d) datum in Figure 4). In the doublet state, the Fe−O distance is 1.969 Å, while in the quartet state it gets longer, 2.237 Å, due to the occupancy of the $\sigma^*(z^2)$ orbital. The $OOH(^-)$ ligand is much more strongly bound to iron than the H_2O_2 ligand, especially for the doublet state. Much like before, for the Fe−OOH complex too, one can clearly see, as illustrated in Figure 5A, that the distal residues, $His(H^+)42$ and Arg38 maintain multiple hydrogen-boding interactions with the OOH moiety.

We tried also to locate the $Fe-OOH_2$ species (Scheme 1). Although the species was not of a high energy, it did not belong to a genuine minimum; during the QM/MM optimization, this species fell apart in two distinct ways, either back to Cpd 0 by transferring the second proton on O_β to the nitrogen of His42, or by splitting a water molecule and forming Cpd I. Apparently, the multiple hydrogen bonding exerted by the two distal residues Arg38 and His42 on the OOH_2^+ moiety apply a strong "pull effect"[1,3,4,6,7] and destabilize the $FeOOH_2^+$ species toward dissociation of a water molecule.

The Acidity of H_2O_2 in the Ferric Complex. As recently argued by Jones and Dunford,[4b] and by Hiner et al.,[7] the pK_a of complexes H_2O_2 is significantly smaller than that of the free hydrogen peroxide. As may be seen from Figures 3 and 4, the energy difference between the ferric(H_2O_2)/His42 and the ferric-hydroperoxide/His42-H^+ complexes is very small, signifying the increased acidity of the complex's hydrogen peroxide. At the UB3LYP/B1 and UB3LYP/B1+d levels the deprotonation is slightly exothermic (−3.5 and −0.7 kcal/mol, respectively), with B2 the reaction is slightly endothermic (+2.4 kcal/mol relative to the quartet spin state of the $Fe(H_2O_2)$ species), while with B3 it is slightly exothermic by −0.4 kcal/mol. We can take the latter value as our "best" one, since the B3 basis set is quite large and balanced (having polarization and diffuse

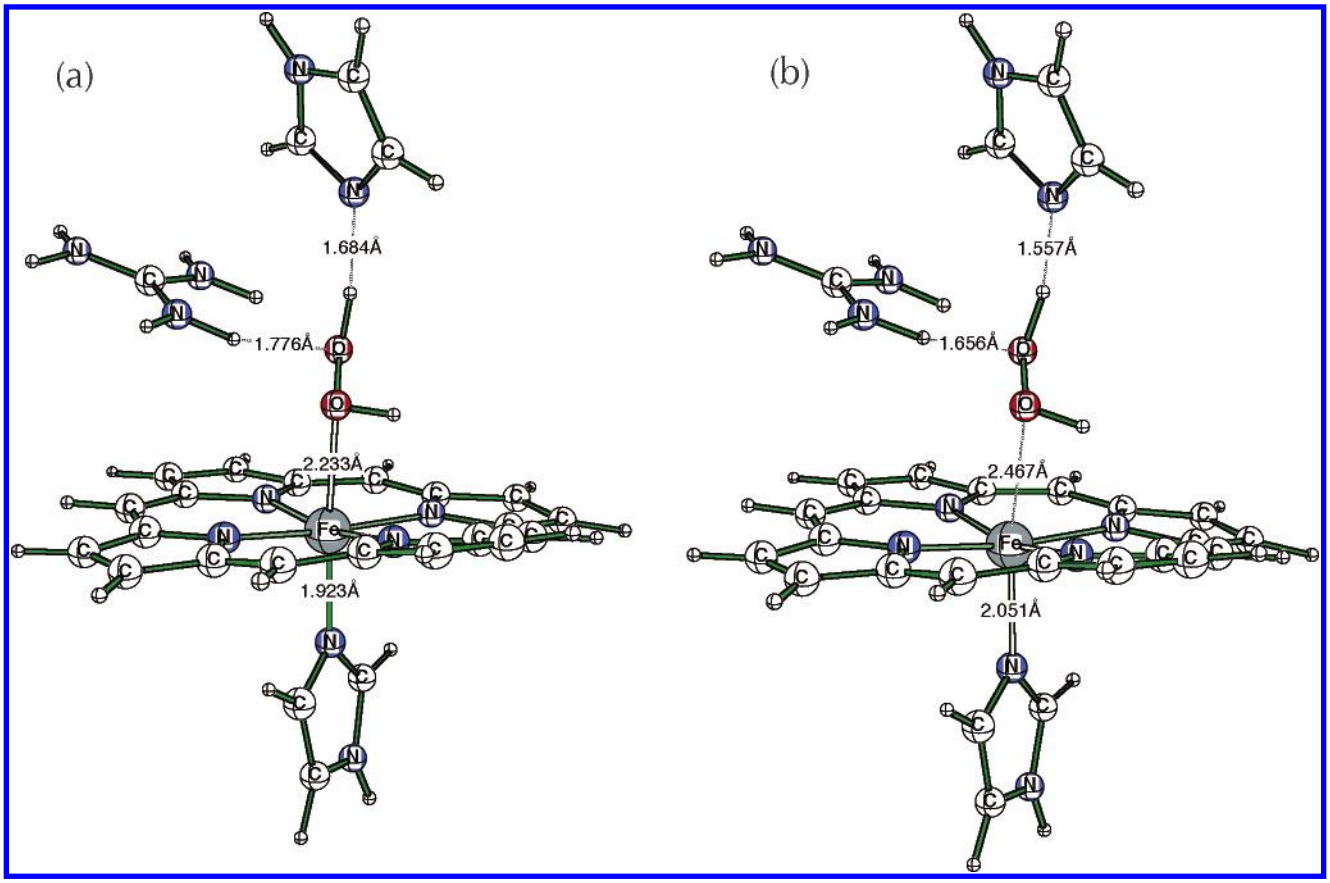

Figure 2. QM subsystem of the QM/MM model for the complex of HRP with H_2O_2 in the (a) doublet state and (b) quartet state, optimized at the UB3LYP/B1+(d):CHARMM level.

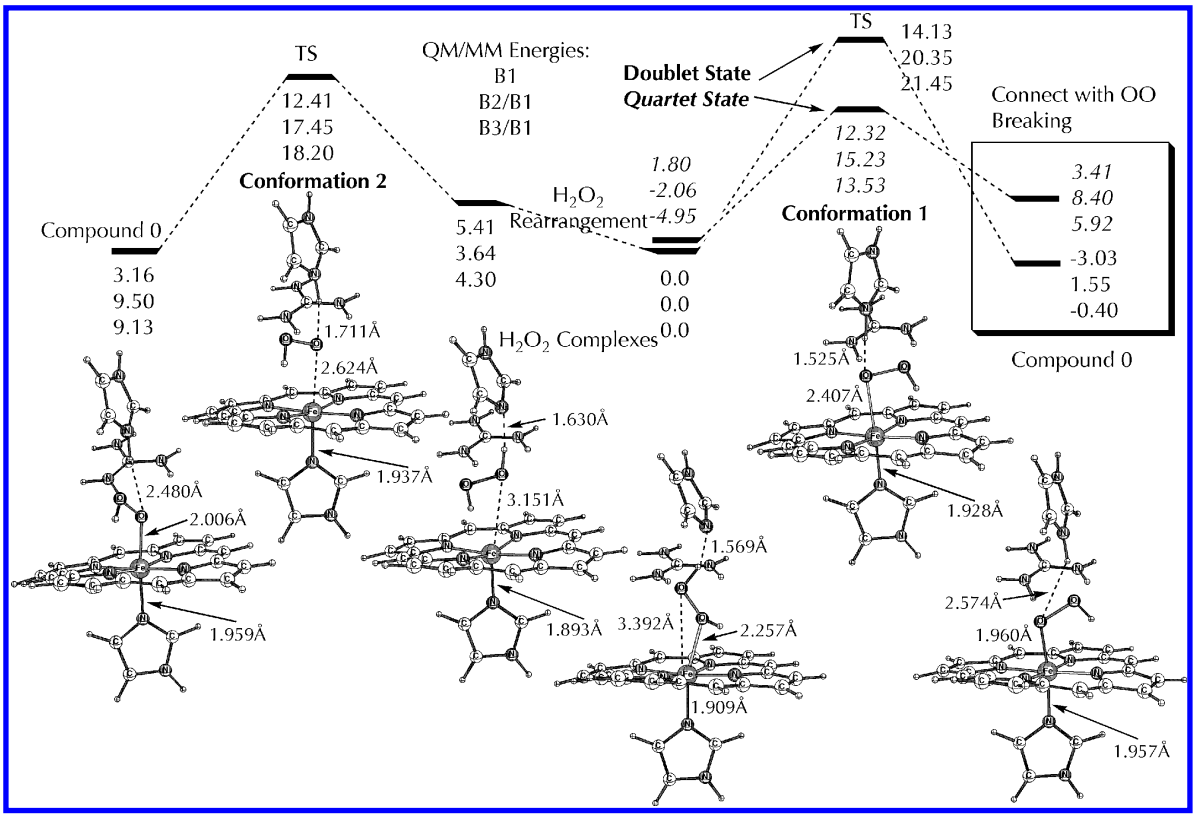

Figure 3. Energy profiles for the two deprotonation mechanisms of the Fe(H_2O_2) complex, calculated at the UB3LYP:CHARMM with different basis sets. Important bond distances for the doublet are given on the structures. The doublet and quartet spin state surfaces are shown.

functions on the organic moieties as well). Thus, within the accuracy of QM/MM calculations the complexed H_2O_2 becomes a reasonably strong acid and can thermodynamically transfer a proton to imidazole.

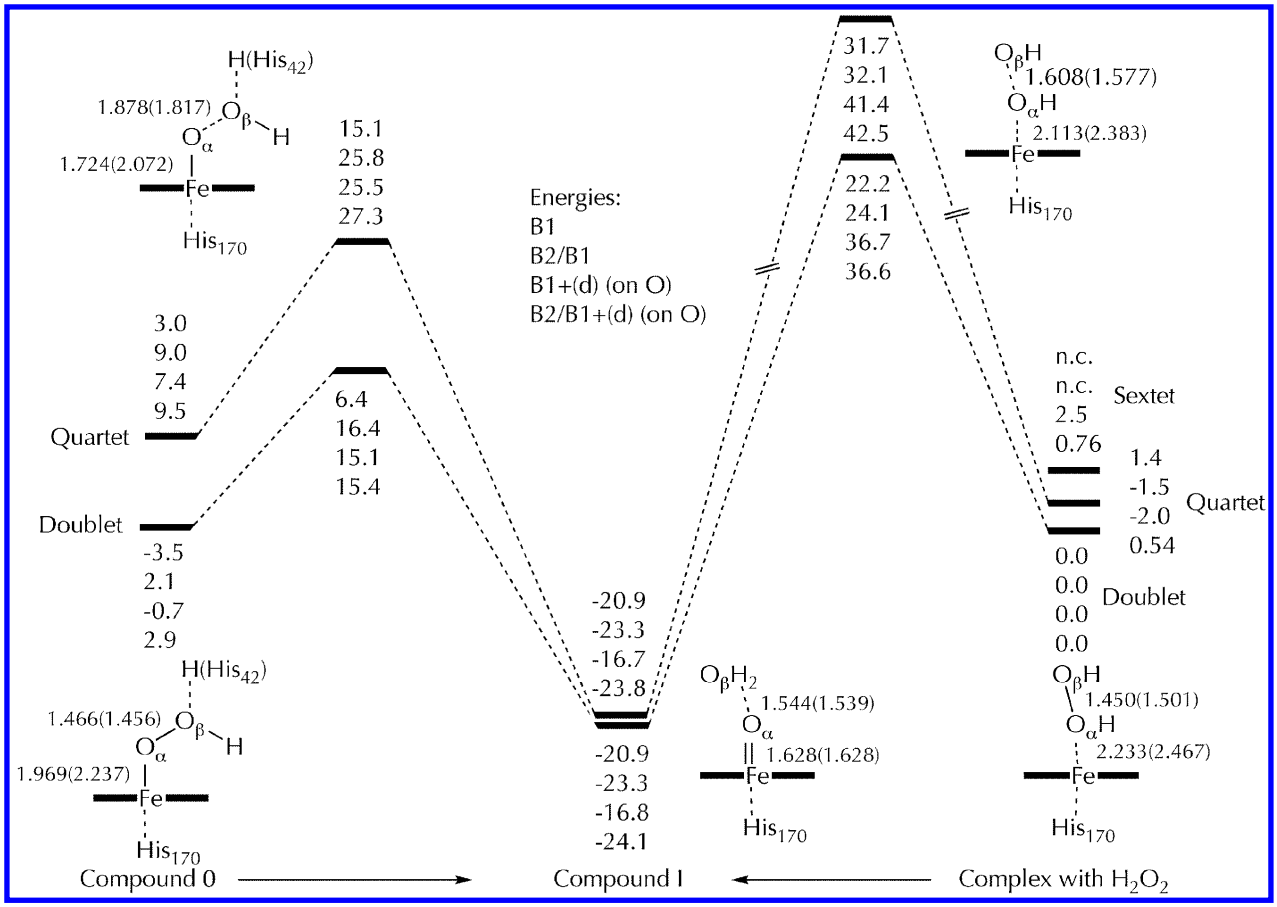

Figure 4. Energy profiles for the two competing mechanisms of formation of Compound I, calculated at the UB3LYP:CHARMM with different basis sets. Important bond distances for the doublet (quartet) are given on the schematic structures.

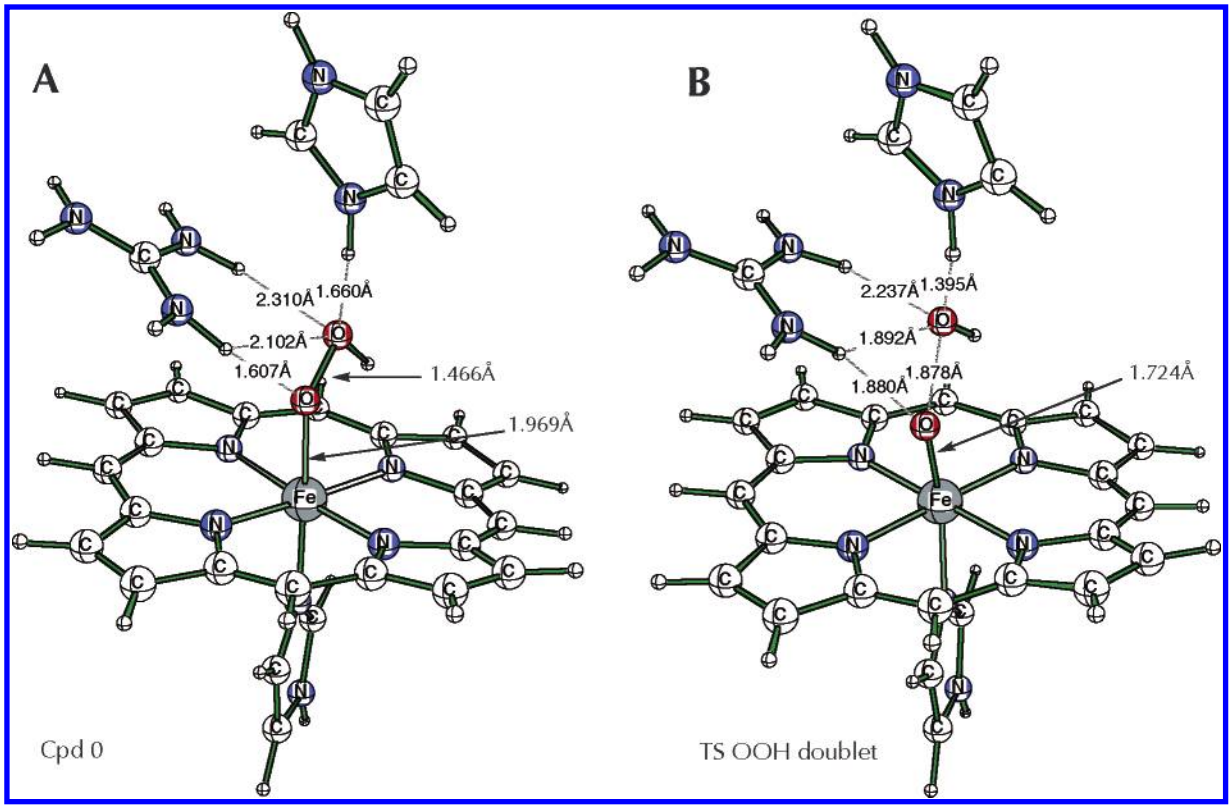

Figure 5. (A) Calculated Cpd 0 showing the hydrogen network with Arg38 and His42. (B) Optimized transition state for Cpd I formation from Cpd 0 showing the tightening of the hydrogen-bonding network. Data obtained in the doublet state at the UB3LYP/B1+(d):CHARMM level.

We have made many attempts to find a pathway for this proton transfer, and these attempts are summarized in the Supporting Information (pages S.37−S.40). The major problem of finding a low energy transition state for the process are the

following. (a) His42 that has to act as a base is 3.819 Å (H_2O_2 complex with B1 in the doublet state) away from the proximal proton of H_2O_2, and this leads to a high barrier. (b) The active site is tight and has no space for an additional water molecule to enter in and shuttle the proton transfer. (c) QM calculations, using a model system including the residues H42 and Arg38, show that deprotonation of the distal proton of H_2O_2 is extremely facile, in fact barrier free (see Supporting Information page S.39); however, the follow-up rearrangement of the Fe−O(H)-O^- species led to very high barrier (Supporting Information page S.39). In the QM/MM calculations we could not locate the Fe−O(H)−O^- species (Supporting Information page S.40).

Since Arg38 is placed in an ideal position to assist the deprotonation of the proximal hydrogen, we ran a QM/MM energy scan starting from His42-H^+ and Arg38-neutral. In this case (Supporting Information page S.41) the neutral Arg abstracted the proton in a barrier free fashion. We, however, have to discard this mechanism since the experimentally estimated pK_a of Arg38 is ∼14, compared with 2.5−3.8 for His42-H^+.[4,7]

The most reasonable mechanism we found is depicted in Figure 3. Thus, starting from Fe(H_2O_2) in the middle, and moving to the left, the complex may rearrange the conformation of H_2O_2 and release the latter molecule so it approaches His42. From this conformation, the proximal H is deprotonated, leading first to a nonrelaxed FeOOH isomer, which of course relaxes subsequently to the most stable conformation (this relaxation is not shown in the figure but can be appreciated by comparing the energies of Cpd 0 in the left-hand side with the one at the right-hand; the latter is the relaxed species). The total barrier for this doublet state process is reasonable with B1, 12.4 kcal/mol, 17.5 kcal/mol with B2, and 18.2 kcal/mol with B3. Moving now to the right, the distal proton is transferred simultaneously with a flip of the Fe−OHO moiety to the Fe−OOH connectivity. Once again, the barrier on the doublet state surface with B1 is reasonable; with B2 and B3 it is 20.4−21.5 kcal/mol.

Since the Fe−O bond in Fe−(H_2O_2) is longer in the quartet state, the hydrogen peroxide is closer to His42, and we therefore expected that the deprotonation would have a lower barrier on the quartet surface. This is indeed the case in Figure 3; the barrier is ca. 3 kcal/mol lower than on the doublet surface (with B3: barrier of 18.5 kcal/mol). In such a case, the deprotonation will occur with spin crossover from the quartet to the doublet state. With both B2 and B3, the ground state of the Fe(H_2O_2) complex is the quartet state, so the reaction will anyway have to start on this spin state with a subsequent crossover to the doublet surface. This is not forbidden, since the spin−orbit coupling between the two states of FeOOH is expected to be significant.[26]

In sum, the barriers for deprotonation are in the range of 12−17 kcal/mol, depending on the basis set. If we consider that zero point energy correction is ca. 3 kcal/mol, then the barriers will be still lower by this amount, i.e., 9−14 kcal/mol. The experimental data show a total free energy barrier for the formation of Cpd I is approximately 13 kcal/mol (rate constant of 1200 s^{-1}).[7a] Thus within the limitations of the QM(DFT)/MM calculations the correspondence to experimental data is fair.

Reaction Mechanisms for Heterolytic O−O Bond Cleavage. Both the Fe(H_2O_2) and Cpd 0 species can, in principle, serve as starting points for the formation of Cpd I. These mechanisms are traced in Figure 4 and feature in each case two well separated spin state surfaces; no spin-state crossing was observed during the QM/MM energy scans. The first mechanism is nascent from Fe(H_2O_2) and follows from right to the middle of the Figure: the proton bonded to O_α migrates to O_β, and a water molecule splits off to form directly Cpd I. In the doublet state, the barrier is 36.6 kcal/mol (B2/B1+(d)) and in the quartet state 42.5 kcal/mol; both values are not too far from the O−O bond dissociation energy of H_2O_2, which is around 51 kcal/mol.[27] The height of this barrier is due to the fact that the 1,2-proton migration is a "forbidden" process.[28] Thus, despite the presence of the Arg38 and His42 residues, this 1,2-proton shift path has high barriers, and the respective mechanism can be ruled out, at least under conditions of neutral-to-basic pH.

The mechanism of formation of HRP Cpd I from Cpd 0 is an alternative and follows the energy profile from left to the middle of Figure 4. The Cpd 0 species itself is generated after deprotonation of the proximal OH of H_2O_2 by the His42 residue, as described above in some detail. Moreover, now in the doublet state, the barrier at the best level available here, B2/B1+(d), is only 12.5 kcal/mol. Zero point energy is expected to further lower this value, leading to reasonably fast formation of Cpd I. In the quartet case, the barrier is significantly higher (17.8 kcal/mol). And since the quartet state of Cpd 0 is 6.6 kcal/mol higher than the doublet state, the deprotonation and O−O bond breaking will occur primarily via the doublet state; the quartet state of Cpd I may subsequently be generated by spin crossover or spin equilibrium. No spin-state crossing, as reported[12a] in studies of isolated model systems or synthetic reagents, was observed in our study.

In sum, the heterolytic cleavage nascent from Cpd 0 has a much lower energy barrier than the one initiated from ferric-hydrogen peroxide. Cpd 0 in turn is formed by the deprotonation of the ligated H_2O_2 by His42; the barriers for the two processes are roughly comparable. This result highlights the crucial role of the His42 that acts as a base to deprotonate the hydrogen peroxide and generates the key species in the low energy mechanism. The role of His42 has been well recognized and supported by site directed mutation studies of the distal residues.[1,3,6,7] Nevertheless, as is discussed below the Arg38, while not crucial for the deprotonation of H_2O_2 or to the O−O activation, plays an important role by lowering barrier for the heterolytic bond cleavage.

Electronic Reorganization During Heterolytic Cleavage. We recall that the formation of Cpd I from Cpd 0 involves heterolytic O−O cleavage that entails a change of the oxidation states by two oxidation equivalents, from PorFe(III)−OOH/His42-H^+ to $Por^{+\bullet}$Fe(IV)═O/H_2O;His42. Clearly, according to Figure 4, the environment of the active site of HRP, reduces drastically the barrier for this heterolytic O−O bond cleavage, and enables thereby the formation of Cpd I. This lowering of the barrier for heterolytic cleavage is achieved by a cooperative effort of the distal residues. A simple quantum mechanical rationale for the heterolytic cleavages of O−O bonds was given before by Bassan et al.[12b] Thus, to form Cpd I, from PorFe(III)−OOH, two electrons will have to shift from the heme (PorFe) into the σ^* orbital of the $O_\alpha-O_\beta$ bond and cause its heterolytic cleavage to Por(+•)Fe(IV)O/OH− (note that one electron is added to the oxo group of the FeO moiety which becomes formally a O^{2-} species, and the other electron is added to the OH group that departs as OH−). This electron flow[4b] is promoted by the two positively charged residues, Arg38 and His(H^+)42, which stabilize the $Fe^{IV}O^{2-}$ moiety and the hydroxide ion formation. Structurally, this is illustrated by the QM/MM structure of the transition state in Figure 5B. Thus, comparison to Figure 5A shows that in the transition state, shown in Figure 5B, the two hydrogen-bonding distances of

Arg38 to the departing $O_\beta H^-$ tighten compared with the situation in Cpd 0. Accordingly, the Arg38 "pulls" the $O_\beta H^-$ moiety, while His42(H^+) protonates it to form a water molecule, which eventually departs to bridge the two residues as W427 (Figure 1).

In sum, the mechanism of Cpd I formation in HRP in neutral to basic pH involves two intermediates. The initial complex Fe-(H_2O_2) undergoes deprotonation by His42 to form the ferric-hydroperoxide complex, Cpd 0; this process is likely to involve spin crossover from the doublet to the quartet state (Figure 3), the barrier in the quartet state is calculated to be 18.5 kcal/mol (at the best level, B3). Subsequently, the OH− group of Cpd 0 is pulled by Arg38 and gets reprotonated by His42(H^+) to form a water molecule, W247, that bridges the two residues. The barrier for this second step on the doublet spin state surface is only 12.5 kcal/mol. Zero point energy corrections will lower the first barrier by 3 kcal/mol relative to the second one. Still, however, the rate-limiting step in the formation of HRP Compound I would be the first hydrogen abstraction and not the O−O bond breaking. Even with the highest barrier calculated for the deprotonation of the H_2O_2 molecule, our results suggest that this mechanism will prevail over the 1,2-proton shift mechanism that converts Fe(H_2O_2) to Cpd I.

The Cpd I species in Figure 1, generated via Cpd 0, involve a neutral His42 residue and hence the FeO bond lengths are significantly shorter (see Figure 1) than the Cpd I species computed previously,[14] with the nearby protonated His42-H^+ residue. Thus our results suggest that the nature of Cpd I in HRP depends on the pH. At acidic pH, His42 that lies near the surface can easily be protonated leading to the Cpd I species with a long Fe═O bond,[14] while at neutral and/or basic pH values the species will be like the one shown here in Figure 1 with a shorter Fe═O bond. These differences and the presence or absence of the protonated His42-H^+ residue are likely to affect the reactivity of Cpd I.[4]

Conclusions

The QM/MM calculations of the O−O bond activation in the enzyme HRP, in neutral to basic pH, reveal two alternative mechanisms for the formation of Compound I (Cpd I). One is nascent from the ferric-hydrogen peroxide intermediate and the other from the ferric-hydroperoxide (PorFe−OOH), so-called Cpd 0. The ferric−hydrogen peroxide complex can undergo directly 1,2-proton shift and heterolytic cleavage to form Cpd I. However, this mechanism has a high barrier and is therefore ruled out in the wild-type enzyme.

A low energy mechanism can be initiated first by deprotonation of hydrogen peroxide and then O−O bond heterolysis of the Cpd 0 species. Thus, the acidity of complexed H_2O_2 is enhanced significantly by the coordination to iron and in the presence of Arg38.[4b,7] In this manner Fe(H_2O_2) can transfer the proximal proton to His42; the lowest energy process occur via the quartet spin state with a subsequent crossover to the doublet state of Cpd 0 (Figure 3). Thereafter, His42-H^+ relays the proton to the distal oxygen of Cpd 0 and leads to simultaneous heterolytic cleavage of the O−O bond, generating Cpd I and W427. The positively charged Arg38 facilitates the heterolysis of the bond by "allowing the electrons to flow" from the heme into the O−O bond and releasing an OH^- moiety that gets protonated to H_2O.

As such, the role of the His42 residue is crucial, since it is required to deprotonate the hydrogen peroxide and form Cpd 0, thereby opening the low energy route to Cpd I formation. In this low energy mechanism the Arg38 residue plays an important role by providing hydrogen bonding and a localized positive charge, which assist the occurrence of the heterolytic cleavage. All in all, these results affirm the Poulos−Kraut mechanism[6] and other experimental conclusions.[3,4,7] Theory, however, complements experiment by providing a clear description of all relevant intermediates and lucid insight into the electronic reorganization during heterolytic cleavage and the role of the distal residues in this mechanism.

Acknowledgment. The research was supported in part, by the German Federal Ministry of Education and Research (BMBF) within the framework of the German−Israeli Project Cooperation (DIP) and the Israel Science Foundation (ISF).

Supporting Information Available: Energies, charges, spin densities data, and *xyz* coordinates (QM part) of all calculated species (PDF). This material is available free of charge via the Internet at http://pubs.acs.org.

References and Notes

(1) Poulos, T. L. Peroxidases and Cytochrome P450 in *The Porphyrin Handbook*; Kadish, K. M., Smith, K. M, Guilard, R., Eds.; Academic: New York, 2000; Volume 4, Chapter 32, pp 189−218.

(2) Colas, C.; Ortiz de Montellano, P. R. *Chem. Rev.* **2003**, *103*, 2305−2332.

(3) Sono, M.; Roach, M. P.; Coulter, E. D.; Dawson, J. H. *Chem. Rev.* **1996**, *96*, 2841−2887.

(4) (a) Dunford, H. B. *Heme Peroxidases*, Wiley-VCH: New York, 1999. (b) Jones, P.; Dunford B. *J. Inorg. Biochem.* **2005**, *99*, 2292−2298.

(5) Denisov, I. G.; Makris, T. M.; Sligar, S. G.; Schlichting, I. *Chem. Rev.* **2005**, *105*, 2253−2278.

(6) Poulos, T. L.; Kraut, J. *J. Biol. Chem.* **1980**, *255*, 8199−8205.

(7) (a) Hiner, A. N. P.; Raven, E. L.; Thorneley, R. N. F.; Garcia-Canovas, F.; Rodriguez-Lopez, J. N. *J. Inorg. Biochem.* **2002**, *91*, 27−34. (b) Rodriguez-Lopez, J. N.; Loew, D. J.; Hernandez-Ruiz, J.; Hiner, A. N. P.; Garcia-Canovas, F.; Thorneley, R. N. F. *J. Am. Chem. Soc.* **2001**, *123*, 11838−11847.

(8) de Visser, S. P.; Shaik, S.; Sharma, P. K.; Kumar, D.; Thiel, W. *J. Am. Chem. Soc.* **2003**, *125*, 15779−15788.

(9) (a) Harris, D. L.; Loew, G. H. *J. Porphyrins Phthalocyanines* **2001**, *5*, 334−344. (b) Harris, D. L.; Loew, G. H. *J. Am. Chem. Soc.* **1996**, *118*, 10588−10594. (c) Du, P.; Axe, F. U.; Loew, G. H.; Canuto, S.; Zerner, M. C. *J. Am. Chem. Soc.* **1991**, *113*, 8614−8621.

(10) Rydberg, P.; Sigfridsson, E.; Ryde, U. *J. Biol. Inorg. Chem.* **2004**, *9*, 203−223.

(11) Green, M. T. *J. Am. Chem. Soc.* **2000**, *122*, 9495−9499.

(12) (a) For a QM study of O−O activation in cytochrome *c* peroxidases, see Wistram, M.; Blomberg, M. R. A.; Siegbahn, P. E. M. *J. Am. Chem. Soc.* **1999**, *121*, 10178−10185. (b) For a QM study of O−O activation in nonheme complexes, see Bassan, A.; Blomberg, M. R. A.; Siegbahn, P. E. M. *J. Am. Chem. Soc.* **2002**, *124*, 11056−11063. (c) For a QM study of O−O activation in small models, see Woon, D. E.; Loew, G. H. *J. Phys. Chem. A* **1998**, *102*, 10380−10384.

(13) For Car−Parinello study, see Rovira C.; Fita, I. *J. Phys. Chem. B* **2003**, *107*, 5300−5306.

(14) Derat, E.; Cohen, S.; Shaik, S.; Altun, A.; Thiel, W. *J. Am. Chem. Soc.* **2005**, *127*, 13611−13621.

(15) Berglund, G. I.; Carlsson, G. H.; Smith, A. T.; Szoeke, H.; Henriksen, A.; Hajdu, J. *Nature* **2002**, *417*, 463−468.

(16) Schünemann, V.; Winkler, H. *Rep. Prog. Phys.* **2000**, *63*, 263−353.

(17) Aqvist, J.; Warshel, A. *Chem. Rev.* **1993**, *93*, 2523−2544.

(18) Gao, J. In *Reviews in Computational Chemistry*; Lipkowitz, K. B., Boyd, D. B., Eds.; VCH: Weinheim, 2000; Vol. 7, p 119.

(19) Bakowies, D.; Thiel, W. *J. Phys. Chem.* **1996**, *100*, 10580−10594.

(20) Sherwood, P.; de Vries, A. H.; Guest, M. F.; Schreckenbach, G.; Catlow, C. R. A.; French, S. A.; Sokol, A. A.; Bromley, S. T.; Thiel, W.; Turner, A. J.; Billeter, S.; Terstegen, F.; Thiel, S.; Kendrick, J.; Rogers, S. C.; Casci, J.; Watson, M.; King, F.; Karlsen, E.; Sjovoll, M.; Fahmi, A.; Schafer, A.; Lennartz, C. *J. Mol. Struct. (THEOCHEM)* **2003**, *632*, 1−28.

(21) Ahlrichs, R.; Bär, M.; Häser, M.; Horn, H.; Kölmel, C. *Chem. Phys. Lett.* **1989**, *162*, 165−169.

(22) Smith, W.; Forester, T. *J. Mol. Graph.* **1996**, *14*, 136−141.

(23) MacKerell, A. D., Jr.; Bashford, D.; Bellott, M.; Dunbrack, R. L., Jr.; Evanseck, J. D.; Field, M. J.; Fischer, S.; Gao, J.; Guo, H.; Ha, S.; Joseph-McCarthy, D.; Kuchnir, L.; Kuczera, K.; Lau, F. T. K.; Mattos, C.;

Michnick, S.; Ngo, T.; Nguyen, D. T.; Prodhom, B.; Reiher, W. E., III.; Roux, B.; Schlenkrich, M.; Smith, J. C.; Stote, R.; Straub, J.; Watanabe, M.; Wiórkiewicz-Kuczera, J.; Yin, D.; Karplus, M. *J. Phys. Chem. B* **1998**, *102*, 3586−3616.

(24) LACVP is derived from LANL2DZ: Hay, J. P.; Wadt, W. R. *J. Chem. Phys.* **1985**, *82*, 299−310.

(25) Wachters, A. J. H. *J. Chem. Phys*. **1970**, *52*, 1033−1036.

(26) Danovich, D. and Shaik, S. *J. Am. Chem. Soc.* **1997**, *119*, 1773−1786.

(27) Kerr, J. A. *Chem. Rev.* **1966**, *66*, 465−500.

(28) Woodward, R. B. and Hoffmann, R. *The conservation of orbital symmetry*; Verlag-Chemie; Weinheim, 1970.